Published in final edited form as:

Cell Mol Neurobiol. 2012 May ; 32(4): 613–624. doi:10.1007/s10571-012-9808-4.

Cell Selective Conditional Null Mutations of Serine Racemase Demonstrate a Predominate Localization in Cortical Glutamatergic Neurons

Michael A. Benneyworth,
McLean Hospital, MRC 114, 115 Mill St., Belmont, MA 02478, USA

Yan Li,
McLean Hospital, MRC 206, 115 Mill St., Belmont, MA 02478, USA

Alo C. Basu,
McLean Hospital, MRC 117, 115 Mill St., Belmont, MA 02478, USA

Vadim Y. Bolshakov, and
McLean Hospital, MRC 209, 115 Mill St., Belmont, MA 02478, USA

Joseph T. Coyle
McLean Hospital, MRC 122, 115 Mill St., Belmont, MA 02478, USA

Joseph T. Coyle: Joseph_Coyle@hms.harvard.edu

Abstract

D-Serine, which is synthesized by the enzyme serine racemase (SR), is a co-agonist at the *N*-methyl-D-aspartate receptor (NMDAR). Crucial to an understanding of the signaling functions of D-serine is defining the sites responsible for its synthesis and release. In order to quantify the contributions of astrocytes and neurons to SR and D-serine localization, we used recombinant DNA techniques to effect cell type selective suppression of SR expression in astrocytes (*a*SRCKO) and in forebrain glutamatergic neurons (*n*SRCKO). The majority of SR is expressed in neurons: SR expression was reduced by ~65% in *n*SRCKO cerebral cortex and hippocampus, but only ~15% in *a*SRCKO as quantified by western blots. In contrast, *n*SRCKO is associated with only modest decreases in D-serine levels as quantified by HPLC, whereas D-serine levels were unaffected in *a*SRCKO mice. Liver expression of SR was increased by 35% in the *n*SRCKO, suggesting a role for peripheral SR in the maintenance of brain D-serine. Electrophysiologic studies of long-term potentiation (LTP) at the Schaffer collateral–CA1 pyramidal neuron synapse revealed no alterations in the *a*SRCKO mice versus wild-type. LTP induced by a single tetanic stimulus was reduced by nearly 70% in the *n*SRCKO mice. Furthermore, the mini-excitatory post-synaptic currents mediated by NMDA receptors but not by AMPA receptors were significantly reduced in *n*SRCKO mice. Our findings indicate that in forebrain, where D-serine appears to be the endogenous co-agonist at NMDA receptors, SR is predominantly expressed in glutamatergic neurons, and co-release of glutamate and D-serine is required for optimal activation of post-synaptic NMDA receptors.

Correspondence to: Joseph T. Coyle, Joseph_Coyle@hms.harvard.edu.

Keywords

NMDA receptor; Glycine modulatory site; D-Serine; Serine racemase; Astrocyte; Neuron

Introduction

Once assumed to be limited to invertebrates, D-amino acids, are now established as mediators and modulators of neuronal activity in mammals (Boehning and Snyder 2003; Wolosker et al. 2008). In the case of D-serine, interest in its neurobiology followed the discovery of substantial D-serine levels in the mammalian forebrain (Hashimoto et al. 1993). Binding of glycine or D-serine to the glycine modulatory site on the NR1 subunit of the *N*-methyl-D-aspartate receptor (NMDAR) increases receptor affinity for glutamate and is required for channel opening (Fadda et al. 1988). NMDAR's requirement for the simultaneous action of two separate agonists, perhaps unique in neurobiology, may function as an endogenous protective mechanism against the excitotoxic effects of receptor overactivation (Patel et al. 1990). D-Serine is presumed to be the primary forebrain co-agonist, as it is concentrated in the forebrain, and elimination of synaptic D-serine reduces NMDA receptor-mediated currents (Schell et al. 1995; Mothet et al. 2000).

Understanding the physiological role of D-serine is predicated on the delineation of its synthesis, cellular transport, release and degradation. The cloning and characterization of serine racemase (SR) demonstrated that D-serine is endogenously synthesized in the mammalian brain through the conversion of L- to D-serine (Wolosker et al. 1999). Inactivation of the SR gene reduces cortical D-serine levels by ~85% (Basu et al. 2009). Initial studies using immunostaining methods in rat brain tissue and primary glial cultures suggested that D-serine and SR are principally expressed in astrocytes (Schell et al. 1995; Wolosker et al. 1999). Astrocytic unsheathing of synapses of the supraoptic nucleus is accompanied by a loss in NMDAR-mediated currents in a manner consistent with a loss of synaptic D-serine (Panatier et al. 2006). Primary cultures enriched for astrocytes express SR and release D-serine upon glutamate receptor activation (Schell et al. 1995; Wolosker et al. 1999; Mothet et al. 2005). These findings supported the notion that glia are a primary source of D-serine. However, given the regional heterogeneity of astrocytes and the impact of culture conditions (Zhang and Barres 2010), it is difficult to draw quantitative conclusions about SR expression in glia/astrocytes from tissue culture studies. Furthermore, recent immunohistochemical studies, in which different antibodies were used, have suggested a more prominent neuronal SR expression, consistent with D-serine serving as a traditional neurotransmitter (Kartvelishvily et al. 2006; Miya et al. 2008; Ding et al. 2010).

Given the variability in antibody specificity and the qualitative nature of immunohistochemical and tissue culture data, the absolute amount of SR expressed in forebrain neurons or astrocytes remains unresolved. To address this issue in a quantitative manner, we have employed a genetic strategy to determine the relative expression of SR in neurons and in astrocytes by creating neuron- or astrocyte-specific SR conditional knockout (SRCKO) mice. The first coding exon (exon 3) of the murine SR gene was flanked with loxP sites, and the gene was silenced by cell type specific expression of Cre recombinase.

Materials and Methods

Subjects

All genetic constructs used in these experiments were maintained on a C57BL/6J mouse background (back-crossed ≥10 generations). The genetic constructs used to generate conditional knockouts are shown in Fig. 1. The floxed (fl) SR construct (Fig. 1a) was generated as previously described (Basu et al. 2009). In this construct, the first coding exon (exon 3) is flanked by loxP sites, which results in excision of the intervening sequence upon exposure to Cre recombinase. PCR primer sequences for the SR gene are: tgtgtgaatgtgtcacatac (forward) and acgtgggaacctgctggattct (reverse). Genotyping PCR results in the formation of two distinct products of ~650 and ~750 bp corresponding to the wild-type (+) and floxed SR alleles (Fig. 1d). For astrocyte-specific expression, we used a transgenic mouse line in which Cre recombinase expression was controlled in a cell type specific and inducible way by a promoter element that combined the human glial fibrillary acidic protein (GFAP) promoter and a mutant estrogen receptor (Fig. 1b; Casper et al. 2007), kindly provided by Ken McCarthy (University of North Carolina). The mutant estrogen receptor (ER^{T2}) is activated only in response to the exogenous compound tamoxifen (TAM; Sigma-Aldrich, St. Louis, MO). TAM was administered at daily doses of 40–250 mg/kg (i.p. or s.c.), dissolved in a vehicle of 85% sunflower oil and 15% ethanol, and injected at a volume of 5 mL/kg. In the second Cre transgenic mouse line, which was kindly provided by Yu Yamaguchi (Burnham Institute for Medical Research), Cre expression was driven by a promoter for the α-subunit of Ca^{2+}/calmodulin-dependent kinase II (CaMKIIα; Fig. 1c). This specific transgene (CaMKIICre2834) was previously described to produce Cre expression in forebrain neurons beginning at postnatal day 17 and reaching near adult levels by day 34 (Schweizer et al. 2003). The same PCR primers were used to amplify both Cre transgenes, ggtcgatgcaacgagtgatgagg (forward) and gctaagtgccttctctacacctgcg (reverse), which produced a PCR product of ~600 bp. Astrocyte-specific SRCKO (*a*SRCKO) mice were created by generating mice that expressed the GFAP-$CreER^{T2}$ transgene in mice homozygous for the floxed SR gene (SR fl/fl) and treating them with TAM. Neuron-specific SRCKO (*n*SRCKO) mice were created by generating mice that expressed the CaMKIICre2834 transgene in SR fl/fl mice. With both conditional mutants, the control mice were the SR fl/fl genotype that did not carry the Cre transgene, with the controls for the *a*SRCKO also receiving TAM treatment. When indicated, comparisons to wild-type (WT) controls were also made. Constitutive SR knockout (SRKO) mice (Basu et al. 2009) were also used in these studies to examine the cellular distribution of D-serine following systemic administration of D-serine (300 mg/kg, s.c.; Sigma-Aldrich). Animals were housed in a facility with a 12/12 h light/dark cycle and provided with food and water ad libitum. Principles of humane laboratory animal care were followed, and studies were performed with the approval of the McLean Hospital Institutional Animal Care and Use Committee.

Tissue Dissection and Preparation

Brain dissection for analysis of SR expression and D-serine content in homogenates was performed as previously described (Glowinski and Iversen 1966). For *n*SRCKO experiments, brains were rapidly removed, washed in ice-cold PBS, dissected and flash frozen using isopentane on dry ice. Single hemisphere samples of frontal cortex, striatum

and hippocampus were collected. For *a*SRCKO experiments, forebrain samples were collected (containing cortex, hippocampus and striatum). Four separate tests were performed with different treatment protocols to allow us to determine the dose of TAM and post-treatment interval (1–15 days) necessary to optimize the *a*SRCKO. For analysis of liver tissue in *n*SRCKO subjects, a right lobe of the liver was excised and frozen.

Protein and amino acid analysis was done using tissue homogenate from the same samples. Brain tissue was briefly homogenized by sonication (<10 s) in extraction buffer (60-mM Tris buffer, 2% sodium dodecyl sulfate, pH 6.8). Protein content was determined by a colorimetric assay based upon the Bradford method using Bio-Rad dye reagent (Bio-Rad Life Sciences, Hercules, CA). For analysis of SR expression, protein concentrations were diluted to 1 mg/mL for brain samples and 2 mg/mL for liver samples. For amino acid analysis, protein concentration was adjusted to 1 mg/mL and internal standard (L-homocysteic acid) was added at a concentration of 4 μmol/g protein. Proteins were precipitated from the homogenate using trichloroacetic acid (5% w/v). The samples were centrifuged at 18,000×*g* (30 min at 4°C), and the supernatant was extracted three times with water-saturated diethyl ether.

High-Performance Liquid Chromatography (HPLC)

Amino acids were derivatized with *o*-phthaldialdehyde (Alfa Aesar, Ward Hill, MA) and N-*tert*-butyloxycarbonyl-L-cysteine (Novabiochem, Gibbstown, NJ) as previously described (Hashimoto et al. 1992). Derivatized samples were resolved by a C18 column (Alltima HP C18, 3 μm pore, Grace Discovery Sciences) and analyzed by fluoro-metric detection. The HPLC system consisted of a SCL-10A controller, two LC-10AT VP pumps, a SIL-10AD auto injector, a DGU-20A5 degasser and a RF-551 fluorescence monitor (all instruments by Shimadzu Corporation, Kyoto, Japan). The separation was accomplished by application of a binary gradient of 25-mM sodium acetate (pH 6.5) and acetonitrile. The gradient progressed from 10 to 20% acetonitrile during a 20-min period at a flow rate of 1.0 mL/minute. The column was allowed to re-equilibrate to starting concentrations after each run. This procedure produces a separation of D-serine that is distinct from all other amino acids in the sample and on a flat and stable baseline (Fig. 2c). Both D- and L-serine peaks are fully separated from the intervening glutamine peak. The detection and quantitation limits for D-serine were 0.16 and 0.53 μmol/g protein, respectively. Amino acid concentrations were calculated using the internal standard as a comparison to standard samples run at the beginning of each session, as previously described (Hashimoto et al. 1992).

Immunoblotting

Protein samples (20 μg/lane brain samples or 40 μg/lane liver samples) were separated by electrophoresis on 15% acrylamide gels under denaturing and reducing conditions and transferred to nitrocellulose membranes. Primary antibodies were: goat α SR (1:800; sc5751, Santa Cruz Biotechnology, Santa Cruz, CA) and rabbit α β-actin (1:8 K; ab8227; Abcam, Cambridge, MA). Secondary antibodies used were: rabbit αgoat (1:5 K; sc2768, Santa Cruz Biotechnology, Santa Cruz) and goat αrabbit (1:5 K ab6721, Abcam). Proteins were visualized with chemiluminescence (Western Lightning Reagent, PerkinElmer; Waltham, MA). Protein band intensity was determined by densitometry (Quantity One, BioRad;

Hercules, CA). SR expression was normalized to β-actin for each sample (except in the brain vs. liver comparison), normalized to the control condition and averaged across replicate experiments.

Immunohistochemistry

Tissue for immunohistochemical studies was obtained from transcardially perfused mice. Subjects were deeply anesthetized with pentobarbital (180 mg/kg, s.c.) and perfused with 0.1-M phosphate-buffered saline followed by fixative (in 0.1-M phosphate buffer, pH 7.4). Brains were post-fixed for 24 h in the fixative and cryoprotected in increasing concentrations of sucrose (15 and 30%). Immunohistochemistry was performed on 40 μm free-floating sagittal sections, which were cut using a freezing-stage microtome. SR was localized using a primary antibody of mouse origin (1:2K, 61053, BD Biosciences) diluted in phosphate-buffered saline with 3.0% bovine serum albumin and 0.1% Triton X-100. Tissue sections were incubated with biotinylated secondary antibody raised against the primary antibody host species (1:1K; horse anti-mouse (BA-2000) or goat anti-rabbit (BA-1000), Vector Laboratories; Burlingame, CA) and ABC reagent (ABC Elite kit, Vector Laboratories). Colorimetric detection was performed with 3,3-diam-inobenzidine (0.02%) enhanced with nickel(II) sulfate (0.08%) in 0.01-M phosphate buffer. Experimental and corresponding control samples were processed in parallel. Immunostaining was visualized on a Ziess Axioskop microscope using StereoInvestigator software (MBF Bioscience; Welliston, VT) to capture the digital images under constant conditions for subjects of each comparison. In the case of the images containing cortex and hippocampus, multiple overlapping images were brought into register using Photoshop CS5 (Adobe Systems Inc., San Jose, CA) to create the resulting collage images.

Electrophysiology

Hippocampal slices (350–400 μm) were prepared from 14- to 18-week-old *n*SRCKO or *a*SRCKO mice and their control littermates. Slices were continuously superfused in solution containing (in mM): 119 NaCl, 2.5 KCl, 2.5 CaCl2, 1.0 MgSO4, 1.25 NaH2PO4, 26.0 NaHCO3, 10 glucose and 0.05 picrotoxin and equilibrated with 95% O_2 and 5% CO_2 (pH 7.3–7.4) at room temperature (22–24°C). Field potentials (fEPSPs) were recorded in stratum radiatum of the CA1 region with a glass recording electrode (3–4 MΩ resistance) filled with extracellular solution. Baseline synaptic responses were evoked once every 30 s by stimulation of Schaffer collaterals with concentric stimulation electrodes (Shin et al. 2006). Stimulation electrodes were positioned in stratum radiatum more than 200 μm away from the recording electrode. In all LTP experiments, the stimulus intensity was adjusted to produce baseline synaptic responses with an amplitude of ~0.5 mV (100 μs, 2–5 V). LTP was induced with one or three 1-s trains of 100 Hz stimulation. Multiple stimulation trains were delivered 20 s apart. The initial slope of the rising phase of the fEPSP was used to monitor synaptic strength before and after the induction of LTP. Summary LTP graphs were constructed by normalizing data in 60 s epochs to the mean value of the baseline fEPSP slope. The magnitude of LTP was estimated during a 5-min window at 45 min after the induction. Whole-cell recordings of spontaneous miniature excitatory postsynaptic currents (mEPSCs) were obtained from pyramidal neurons in the CA1 area in the presence of 1.0 μM TTX at physiological temperatures (35–36°C). Patch electrodes (3–4 MΩ resistance)

contained (in mM): 120-mM Cs-methanesulfonate, 5 NaCl, 1 $MgCl_2$, 10 BAPTA, 10 HEPES, 2 MgATP and 0.1 NaGTP (adjusted to pH 7.2 with CsOH). During patch-clamp whole-cell recordings, synaptic currents were filtered at 1 kHz and digitized at 5 kHz. Series resistance was monitored throughout the experiment and was in the range of 10–15 MΩ. The mini-excitatory postsynaptic currents (mEPSCs) were recorded at holding potentials of −70 mV and +40 mV first under control conditions, and then in the presence of 10 μM D-serine in external solution. mEPSCs were analyzed using Mini Analysis program (Synaptosoft Inc.). The results are presented as mean ± SEM.

Statistics

Western blot and HPLC data were analyzed using Student's *t*-test comparisons (*a*SRCKO vs. control forebrain D-serine content and SR expression, *n*SRCKO vs. control liver SR expression and WT brain vs. liver SR content) or two-way analysis of variance (ANOVA) with age and genotype as main effects and Bonferroni-corrected post hoc comparisons between genotypes (*n*SRCKO vs. control D-serine content and SR expression). Electrophysiological data were analyzed for genotype effects using unpaired Student's *t*-test comparisons.

Results

SR Expression and D-Serine Content in the *a*SRCKO

In order to assess the relative contribution of astrocyte-derived SR to D-serine levels in the forebrain, *a*SRCKO mice were generated using a TAM-inducible GFAP+ astrocyte-specific Cre recombinase–mediated knockout of SR gene expression. *a*SRCKO (SR fl/fl, GFAP-$CreER^{T2}$ tg) and control (SR fl/fl) mice were treated with TAM daily for 5 days. Due to uncertainty over the TAM treatment parameters (temporal and dosing) necessary to achieve full astrocytic SR deletion, four experimental conditions were examined: (1) once a day TAM (40 mg/kg) treatment followed by tissue collection 5 or 15 days following the last injection, (2) twice a day TAM (50 mg/kg) treatment followed by tissue collection 5 or 15 days following the last injection, (3) once a day TAM (250 mg/kg) treatment followed by tissue collection 10 days after the last injection and (4) once a day TAM (200 mg/kg) treatment followed by tissue collection 10 days after last injection. Maximum reduction occurred between 10 and 15 days post-injection with no incremental effect of doses greater than 40 mg/kg (the dose used in Casper et al. 2007). Combining these results, SR expression was reduced in forebrain by 15.2% of control (Fig. 2a; $n = 24$; $p < 0.01$) in *a*SRCKO mice. Forebrain tissues from the higher dose (200 and 250 mg/kg) treatment groups were analyzed for D-serine content, and no difference from control was observed (Fig. 2b). D-Serine tissue content of ~4.5 μmol/g protein was consistent with previous findings (Basu et al. 2009). In a control experiment, using a GFAP-lacZ reporter gene (Casper et al. 2007), the TAM treatment used resulted in an 83% reduction in reporter gene expression.

SR Expression and D-Serine Content in the *n*SRCKO

Given the recent immunohistochemical evidence that some SR is localized to neurons, we established a selective genetic suppression of SR in forebrain glutamatergic neurons and quantified the effect of that manipulation on SR expression and D-serine content. Forebrain

neuron-specific deletion of SR in the *n*SRCKO was achieved through the use of a Cre recombinase transgene driven by a CaMKII*α* promoter. We examined the tissue-specific and temporal nature of this conditional deletion through the analysis of SR protein levels in homogenate samples of frontal cortex, hippocampus and striatum in *n*SRCKO (SR fl/fl, CaMKII-Cre2384 tg) and control (SR fl/fl) subjects (Fig. 3). All three brain regions ($n = 5–6$ samples/genotype) showed similar timelines of SR reduction, with minimal or no reductions observed at 4 weeks of age, and the reductions reached a plateau in all brain regions by 12 weeks (Fig. 3a, c, d). Statistical analysis demonstrated an interaction of genotype and age in each of the three brain regions (frontal cortex: $F(2,29) = 7.47$, $p < 0.01$; hippocampus: $F(2,30) = 11.22$, $p < 0.001$; and striatum: $F(2,26) = 4.13$, $p < 0.05$). Bonferroni-corrected post hoc comparisons demonstrated significant differences between *n*SRCKO and control in each brain region at 8 and 12 weeks of age. However, the degree to which SR expression was reduced differed between tissue types, with frontal cortex and hippocampus showing the greatest reductions (−60 and −62%), whereas striatum showed a more modest change (−35%) from control levels. The floxed allele had no effect on SR expression, as determined by comparison of SR fl/fl to WT controls (0.303 ± 0.023 vs. 0.246 ± 0.025, SR/*β*-actin ± SEM, $n = 6$, $p = 0.13$).

Reductions in D-serine content in *n*SRCKO mice were of much smaller magnitude than SR protein expression changes. Tissue content of D-serine was determined by HPLC analysis of amino acid extracts from the same samples used for the immunoblot studies (Fig. 3). Reductions in D-serine content were observed in the frontal cortex (Fig. 3b) and striatum (Fig. 3f), whereas levels were relatively unchanged in the hippocampus (Fig. 3d). Statistical analysis of the frontal cortex data found only a significant main effect of genotype ($F(2,28) = 4.92$, $p < 0.05$), whereas in the striatum, a main effect of age was found ($F(2,29) = 4.57$, $p < 0.05$), as well as a significant interaction between age and genotype ($F(2,29) = 4.49$, $p < 0.05$). In both cases, Bonferroni-corrected post hoc comparisons showed significant differences between *n*SRCKO and control samples at 12 weeks of age ($p < 0.05$). No statistically significant differences were observed in the hippocampus. The floxed allele had no effect on D-serine content, as determined by comparison of SR fl/fl to WT controls (5.04 ± 0.54 vs. 4.90 ± 0.32, μmol/g protein ± SEM, $n = 6$, $p = 0.84$).

Cellular Distribution of SR Expression in Conditional Knockouts

To confirm the cellular specificity of *a*SRCKO and *n*SRCKO mice, we carried out immunohistochemical localization of SR. The observed pattern of staining in the cortex and hippocampus in control subjects (Fig. 4b) is consistent with studies reporting a substantial neuronal localization (Kartvelishvily et al. 2006; Miya et al. 2008). Immunopositive cells of the hippocampus were primarily localized to the principal cell layer, with staining also observed in dendritic arbors lying within the stratum radiatum (Fig. 4e). Immunostaining in the cortex was observed in large cell bodies (Fig. 4f). The morphological characteristics and tissue layer distribution of the SR-immunoreactive cells in the cortex and hippocampus are consistent with expression in pyramidal neurons, and with the pattern reported by Kartvelishvily et al. (2006) using similar methods. Aligning with our immunoblot studies, *a*SRCKO subjects displayed no apparent alteration in the cellular pattern of SR expression (Fig. 4a). Conversely, the *n*SRCKO subjects displayed a prominent reduction in the intensity

and number of immunopositive cells (Fig. 4c). It is noteworthy that the reduction does not seem to affect every SR-expressing cell, as a small number of cells in cortical layers II and IV as well as the principal cell layer of the hippocampus display persistent SR immunoreactivity. Prominent cellular localization of SR was observed throughout the striatum of control subjects (Fig. 4d), which appeared unaffected in either *a*SRCKO or *n*SRCKO (data not shown). The SR primary antibody used in this study was validated in SR knockout mice (not shown), which displayed a complete lack of immunoreactivity, similar to that previously described with another commercially available antibody (Basu et al. 2009).

NMDAR-Dependent LTP Is Suppressed in *n*SRCKO Mice

The mechanisms of NMDAR-dependent synaptic plasticity, specifically LTP, contribute to many crucial cognitive functions (e.g., learning and memory) both under normal and pathological conditions. To differentiate between the roles of D-serine produced by neurons or astrocytes, respectively, in the induction of NMDAR-dependent LTP, we stimulated Schaffer collaterals and recorded field excitatory post-synaptic potentials (fEPSPs) in stratum radiatum of the CA1 area of the hippocampus in slices from *a*SRCKO or *n*SRCKO and littermate control mice. We found that the inducibility of LTP in response to the 1-s train of high-frequency stimulation (100 Hz) was unaffected in slices from *a*SRCKO mice (Fig. 1a, d). Thus, the averaged magnitude of LTP in slices from *a*SRCKO mice (190.3 ± 18.5% of the baseline value, $n = 13$) did not differ from that in slices from control littermate mice (198.9 ± 20.7% of the baseline, $n = 10$; unpaired *t* test, $p = 0.76$ between groups). However, the magnitude of LTP was significantly reduced in slices from *n*SRCKO mice (188.6 ± 9.9%, $n = 9$ of the baseline in slices from control mice and 129.3 ± 5.5%, $n = 10$ in slices from *n*SRCKO mice; significant difference between groups, unpaired *t* test, $p < 0.001$; Fig. 5b, d). There was no difference in the magnitude of LTP in slices from control mice between two groups tested (unpaired *t* test, $p = 0.67$). Interestingly, CA1 LTP in slices from *n*SRCKO mice could be rescued with a stronger induction protocol, implicating three trains of high-frequency stimulation (1 s/100 Hz). Consistent with previous observations, this induction protocol led to significant post-tetanic potentiation (Fig. 5c; Zucker and Regehr 2002). Under these experimental conditions, the magnitude of LTP was not different between control and *n*SRKO mice (unpaired *t* test, $p = 0.73$ between groups). Together, these findings demonstrate the role for neuronal SR expression in the induction of NMDAR-dependent LTP.

Synaptic NMDA Receptor Function in *n*SRCKO Mice

To examine whether the NMDA receptor function is affected in *n*SRCKO mice, we recorded mEPSCs in CA1 pyramidal neurons in slices from mutant mice and their control littermates. The patch-clamp whole-cell recordings were performed at physiological temperatures to enhance the efficiency of the transporter proteins (Asztely et al. 1997). We found that the amplitude of the NMDAR-mediated component of the mEPSC, recorded at a holding potential of +40 mV, was reduced in slices from *n*SRCKO compared to control mice (Fig. 6a, b; control mice: 5.2 ± 0.4 pA, $n = 13$ neurons; *n*SRCKO mice: 3.7 ± 0.5 pA, $n = 10$ neurons; unpaired *t* test, $p = 0.024$), while the AMPAR-mediated current at −70 mV remained unchanged (unpaired *t* test, $p = 0.55$). Subsequent application of D-serine (10 μM) increased the amplitude of the NMDAR mEPSC but not the AMPAR mEPSC in both

groups, providing evidence for the lack of saturation of the NMDAR glycine site under these conditions (Li et al. 2009). In the presence of D-serine, the amplitudes of the NMDAR mEPSCs in slices from *n*SRCKO and control mice did not differ (Fig. 6b; $n = 10$ neurons from control mice, $n = 7$ neurons from *n*SRCKO mice; unpaired *t* test, $p = 0.12$ between groups), indicating that the mutation did not affect the functional properties of NMDA receptors at the studied synapses directly.

Liver SR Expression in the *n*SRCKO

The initial characterization of SR demonstrated that it was also expressed in the liver (Wolosker et al. 1999). However, little attention has been paid to the role of peripheral SR, given the apparently low expression relative to brain. When immunoblot intensity of the SR band is normalized to total protein content within the entire organ [(average band intensity/40 μg protein) × (μg protein/mL homogenized tissue) × (mL homogenized tissue/whole organ)], liver displays a 46% greater total SR expression than the brain (Fig. 7a; $p < 0.05$, Student's *t* test, $n = 8$ samples/organ). Furthermore, liver expression of SR was found to be 35% higher in *n*SRCKO subjects as compared to controls (Fig. 7b; $p < 0.05$, Student's *t* test, $n = 15$ samples/genotype).

Discussion

Previous studies to address the relative cellular localization of SR and its product, D-serine, have relied heavily upon immunostaining procedures in brain tissue and cell culture. However, immunocytochemistry can be limited by a lack of quantitative analysis and issues of epitope cross-reactivity. Additionally, primary cell culture carries with it the caveat that protein expression patterns can be dramatically altered once cells are dissociated from their native environment. This study used a genetic strategy to quantify the cell type specificity of SR expression in the intact brain. The results clearly and quantitatively demonstrate that SR is predominantly expressed in glutamatergic neurons in the mouse forebrain. The selective deletion of SR from neurons results in the greater than 60% reduction of SR expression in cerebral cortex and hippocampus, whereas deletion of SR in astrocytes reduces total expression by less than 20%. The genetics-based and quantitative nature of these findings represent a significant advance beyond previous studies which showed that SR and D-serine are localized to both astrocytes and neurons (Kartvelishvily et al. 2006; Miya et al. 2008; Ding et al. 2010), and stand in contrast to earlier SR and D-serine expression studies that indicated a primarily astrocytic localization (Schell et al. 1995; Wolosker et al. 1999). It is noteworthy that our conditional knockouts do not together account for 100% of SR expression, possibly due to a combination of incomplete penetrance of the Cre transgene, incomplete recombination of the floxed locus in the presence of Cre recombinase and/or compensation at the level of gene regulation. Notably, the *n*SRCKO had a small number of hippocampal principal cells still expressing SR at 12 weeks of age, suggesting that more than 60% of SR is expressed in glutamatergic neurons. In total, our data provide quantitative evidence that the vast majority of SR expression occurs in neurons in the cortex and hippocampus.

Of particular note are the data indicating a substantial disparity between the sites of D-serine synthesis and the cellular levels of D-serine: 60% reduction of SR versus a 33% reduction of D-serine in the frontal cortex; 62% reduction of SR versus a non-significant 14% reduction of D-serine in the hippocampus at 12 weeks in the *n*SRCKO. Only the striatum showed a reduction in D-serine that was comparable to the reduction in SR, and this only after a prolonged decrease in SR. These observations support the argument that neuronal synthesis is not the sole determinant of D-serine levels. One possibility that is not addressed in these studies is alterations to the degradation of D-serine through altered expression of D-amino acid oxidase (DAAO). Another possible explanation for the disparity in the magnitude of change is that neuronal SR also serves to degrade D- and L-serine (through α,β elimination) and that the loss of this degradation partially compensates for the loss of racemase activity (Foltyn et al. 2005; Wolosker 2011). This secondary enzyme activity would limit accumulation of D-serine in neurons, whereas allowing for significant accumulation in astrocytes expressing lower levels of SR (Wolosker 2011).

At the functional level, our results indicate that the ability of synapses in the hippocampus to undergo NMDAR-dependent LTP was impaired in *n*SRCKO mice but it remained intact in mice where SR expression was suppressed only in astrocytes (*a*SRCKO mice) (but see Henneberger et al. 2010). This finding is fully consistent with our observation that SR is predominantly expressed in neurons in forebrain. The LTP deficits in *n*SRCKO mice could be overcome with stronger induction protocols, perhaps reflecting the activity-dependent release of glycine, which can also bind to the NMDAR glycine site and thus support the activation of NMDA receptors (Li et al. 2009) or recruitment of D-serine from astrocytes. As NMDAR-mediated spontaneous synaptic currents were decreased in CA1 hippocampal neurons in *n*SRCKO mice, D-serine originating from neurons may also contribute to tonic activation of NMDARs in the absence of evoked synaptic activity.

Given the observation that SR expression poorly corresponds to D-serine levels in the forebrain, it is conceivable that peripheral sources may also play a role in synthesizing D-serine that is subsequently taken up by the CNS. The initial characterization of SR reported its expression at low levels in the liver, and seemed to disregard this potential source D-serine due to the high systemic DAAO expression (D'Aniello et al. 1993; Wolosker et al. 1999). When the differences in total protein content between brain and liver are taken into account, we found that the liver expresses a higher total amount of SR than the brain. The levels of liver D-serine in adult rats are negligible when the tissue is cleared of blood (Hashimoto et al. 1995), and serum D-serine levels are low but not absent (Hashimoto et al. 1992). Thus, liver may not accumulate D-serine, but it can synthesize it. Furthermore, systemic injection of D-serine results in a rapid increase in brain levels of D-serine that persists long after peripheral levels have declined (Hashimoto and Chiba 2004), demonstrating that D-serine in the peripheral circulation can serve as a source for brain D-serine. The elevation of liver SR in the *n*SRCKO as CNS levels have fallen suggests that there may be cross-talk between the two tissues, possibly to maintain peripheral and brain levels of D-serine. In addition to the potential role as a peripheral source of D-serine, hepatic SR may be involved in other processes such as gluconeogenesis via the α,β elimination activity of the enzyme (Foltyn et al. 2005). More studies are needed to address the functional role of SR in the liver.

Our findings point to a different way of conceptualizing the relationship between D-serine synthesis and function. Given the cellular localization of SR, it seems quite likely that both astrocytes and neurons play roles in regulating D-serine physiology. Cultured astrocytes release D-serine in a glutamate-evoked Ca^{2+}-dependent manner (Mothet et al. 2005). Neurons also demonstrate robust release of endogenous D-serine in tissue culture as well as in acute slice preparations; however, the pharmacology is inconsistent with its localization within neuronal storage vesicles (Rosenberg et al. 2010). Thus, both cell types may provide physiologically relevant pools of D-serine. Our findings indicate that forebrain glutamatergic neurons play the predominant role in D-serine synthesis but that astrocyte SR and possibly liver SR can compensate for the loss of neuronal SR. However, while D-serine levels may be nearly normalized in the hippocampus of the *n*SRCKO mice, the reduced NMDA receptor mEPSCs and the impairment in LTP after a single tetanic stimulus but not after repeated tetanic stimuli suggest that the “compensatory” D-serine is not located in the same neuronal compartment as endogenous D-serine.

Acknowledgments

This work was funded by NIH R01MH051290 and P50MH0G0450. We thank Jiamin Feng and Alexander S. Roseman for animal colony maintenance and genotyping. Cre transgenic mouse strains were generously provided by Yu Yamaguchi and Ken D. McCarthy.

Abbreviations

NMDA	*N*-methyl-D-aspartate
SR	Serine racemase
***a*SRCKO**	Astrocyte-specific SR conditional knockout
***n*SRCKO**	Neuron-specific SR conditional knockout
GFAP	Glial fibrillary acidic protein
TAM	Tamoxifen
CaMKII*α*	*α*-Subunit of Ca^{2+}/calmodulin-dependent kinase II
WT	Wild-type
HPLC	High-performance liquid chromatography

References

Asztely F, Erdemli G, Kullmann DM. Extrasynaptic glutamate spillover in the hippocampus: dependence on temperature and the role of active glutamate uptake. Neuron. 1997; 18:281–293. [PubMed: 9052798]

Basu AC, Tsai GE, Ma CL, Ehmsen JT, Mustafa AK, Han L, Jiang ZI, Benneyworth MA, Froimowitz MP, Lange N, Snyder SH, Bergeron R, Coyle JT. Targeted disruption of serine racemase affects glutamatergic neurotransmission and behavior. Mol Psychiatry. 2009; 14:719–727. [PubMed: 19065142]

Boehning D, Snyder SH. Novel neural modulators. Annu Rev Neurosci. 2003; 26:105–131. [PubMed: 14527267]

Casper KB, Jones K, McCarthy KD. Characterization of astrocyte-specific conditional knockouts. Genesis. 2007; 45:292–299. [PubMed: 17457931]

D'Aniello A, D'Onofrio G, Pischetola M, D'Aniello G, Vetere A, Petrucelli L, Fisher GH. Biological role of D-amino acid oxidase and D-aspartate oxidase. Effects of D-amino acids. J Biol Chem. 1993; 268:26941–26949. [PubMed: 7903300]

Ding X, Ma N, Nagahama M, Yamada K, Semba R. Localization of D-serine and serine racemase in neurons and neuroglias in mouse brain. Neurol Sci. 2011; 32(2):263–267. [PubMed: 20890627]

Fadda E, Danysz W, Wroblewski JT, Costa E. Glycine and D-serine increase the affinity of *N*-methyl-D-aspartate sensitive glutamate binding sites in rat brain synaptic membranes. Neuropharmacology. 1988; 27:1183–1185. [PubMed: 2849731]

Foltyn VN, Bendikov I, De Miranda J, Panizzutti R, Dumin E, Shleper M, Li P, Toney MD, Kartvelishvily E, Wolosker H. Serine racemase modulates intracellular D-serine levels through an alpha, beta-elimination activity. J Biol Chem. 2005; 280:1754–1763. [PubMed: 15536068]

Glowinski J, Iversen LL. Regional studies of catecholamines in the rat brain. I. The disposition of [3H]norepinephrine, [3H] dopamine and [3H]dopa in various regions of the brain. J Neurochem. 1966; 13:655–669. [PubMed: 5950056]

Hashimoto A, Chiba S. Effect of systemic administration of D-serine on the levels of D- and L-serine in several brain areas and periphery of rat. Eur J Pharmacol. 2004; 495:153–158. [PubMed: 15249164]

Hashimoto A, Nishikawa T, Oka T, Takahashi K, Hayashi T. Determination of free amino acid enantiomers in rat brain and serum by high-performance liquid chromatography after derivatization with *N*-*tert*-butyloxycarbonyl-L-cysteine and *o*-phthaldialdehyde. J Chromatogr. 1992; 582:41–48. [PubMed: 1491056]

Hashimoto A, Nishikawa T, Oka T, Takahashi K. Endogenous D-serine in rat brain: *N*-methyl-D-aspartate receptor-related distribution and aging. J Neurochem. 1993; 60:783–786. [PubMed: 8419554]

Hashimoto A, Oka T, Nishikawa T. Anatomical distribution and postnatal changes in endogenous free D-aspartate and D-serine in rat brain and periphery. Eur J Neurosci. 1995; 7:1657–1663. [PubMed: 7582120]

Henneberger C, Papouin T, Oliet SH, Rusakov DA. Long-term potentiation depends on release of D-serine from astrocytes. Nature. 2010; 463:232–236. [PubMed: 20075918]

Kartvelishvily E, Shleper M, Balan L, Dumin E, Wolosker H. Neuron-derived D-serine release provides a novel means to activate *N*-methyl-D-aspartate receptors. J Biol Chem. 2006; 281:14151–14162. [PubMed: 16551623]

Li Y, Krupa B, Kang JS, Bolshakov VY, Liu G. Glycine site of NMDA receptor serves as a spatiotemporal detector of synaptic activity patterns. J Neurophysiol. 2009; 102:578–589. [PubMed: 19439669]

Miya K, Inoue R, Takata Y, Abe M, Natsume R, Sakimura K, Hongou K, Miyawaki T, Mori H. Serine racemase is predominantly localized in neurons in mouse brain. J Comp Neurol. 2008; 510:641–654. [PubMed: 18698599]

Mothet JP, Parent AT, Wolosker H, Brady RO Jr, Linden DJ, Ferris CD, Rogawski MA, Snyder SH. D-Serine is an endogenous ligand for the glycine site of the *N*-methyl-D-aspartate receptor. Proc Natl Acad Sci USA. 2000; 97:4926–4931. [PubMed: 10781100]

Mothet JP, Pollegioni L, Ouanounou G, Martineau M, Fossier P, Baux G. Glutamate receptor activation triggers a calcium-dependent and SNARE protein-dependent release of the glio-transmitter D-serine. Proc Natl Acad Sci USA. 2005; 102:5606–5611. [PubMed: 15800046]

Panatier A, Theodosis DT, Mothet JP, Touquet B, Pollegioni L, Poulain DA, Oliet SH. Glia-derived D-serine controls NMDA receptor activity and synaptic memory. Cell. 2006; 125:775–784. [PubMed: 16713567]

Patel J, Zinkand WC, Thompson C, Keith R, Salama A. Role of glycine in the *N*-methyl-D-aspartate-mediated neuronal cytotoxicity. J Neurochem. 1990; 54:849–854. [PubMed: 2106010]

Rosenberg D, Kartvelishvily E, Shleper M, Klinker CM, Bowser MT, Wolosker H. Neuronal release of D-serine: a physiological pathway controlling extracellular D-serine concentration. FASEB J. 2010; 24:2951–2961. [PubMed: 20371631]

Schell MJ, Molliver ME, Snyder SH. D-Serine, an endogenous synaptic modulator: localization to astrocytes and glutamate-stimulated release. Proc Natl Acad Sci USA. 1995; 92:3948–3952. [PubMed: 7732010]

Schweizer C, Balsiger S, Bluethmann H, Mansuy IM, Fritschy JM, Mohler H, Luscher B. The gamma 2 subunit of GABA(A) receptors is required for maintenance of receptors at mature synapses. Mol Cell Neurosci. 2003; 24:442–450. [PubMed: 14572465]

Shin RM, Tsvetkov E, Bolshakov VY. Spatiotemporal asymmetry of associative synaptic plasticity in fear conditioning pathways. Neuron. 2006; 52:883–896. [PubMed: 17145508]

Wolosker H. Serine racemase and the serine shuttle between neurons and astrocytes. Biochim Biophys Acta. 2011; 1814(11):1558–1566. [PubMed: 21224019]

Wolosker H, Blackshaw S, Snyder SH. Serine racemase: a glial enzyme synthesizing D-serine to regulate glutamate-*N*-methyl-D-aspartate neurotransmission. Proc Natl Acad Sci USA. 1999; 96:13409–13414. [PubMed: 10557334]

Wolosker H, Dumin E, Balan L, Foltyn VN. D-Amino acids in the brain: D-serine in neurotransmission and neurodegeneration. FEBS J. 2008; 275:3514–3526. [PubMed: 18564180]

Zhang Y, Barres BA. Astrocyte heterogeneity: an underappreciated topic in neurobiology. Curr Opin Neurobiol. 2010; 20:588–594. [PubMed: 20655735]

Zucker RS, Regehr WG. Short-term synaptic plasticity. Annu Rev Physiol. 2002; 64:355–405. [PubMed: 11826273]

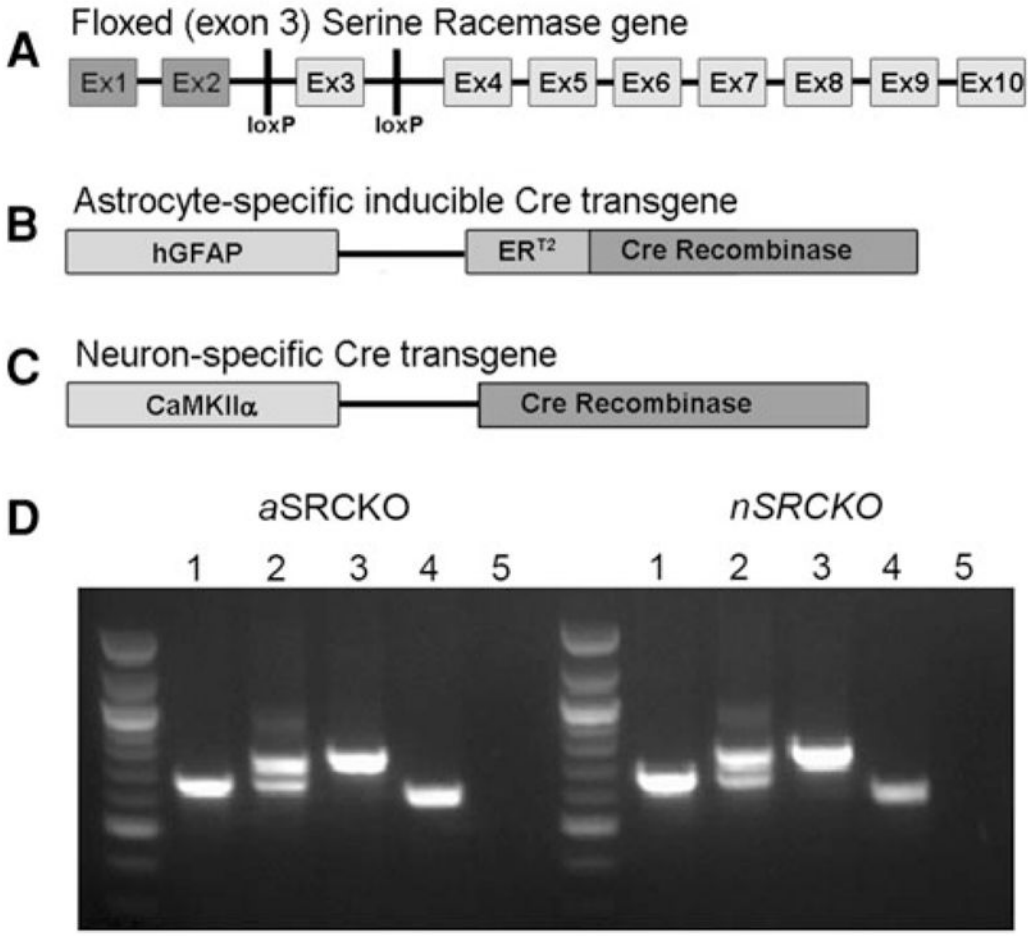

Fig. 1.

Genetic strategy for the creation of *a*SRCKO and *n*SRCKO. Panel **a** shows the "floxed" (fl) SR gene, with loxP sites having been inserted into intronic sequences flanking exon 3. Exons 1 and 2 (*darkly shaded*) are non-coding. Panels **b** and **c** illustrate the promoter elements (*lighter shading*) of the Cre recombinase transgenes that engender cell type specificity, and in the case of **b**, temporal control through TAM induction via the mutant estrogen receptor (ER^{T2}). The glial fibrillary acidic protein (GFAP) promoter is selectively activated in astrocytes and the Ca^{2+}/calmodulin-dependent kinase IIα (CaMKIIα) promoter in neurons of the forebrain. Panel **d** illustrates the genotyping PCR products that identify the various genotypes. For both strains: (1) SR +/+, (2) SR fl/+, (3) SR fl/fl, (4) Cre transgene positive, and (5) no Cre transgene

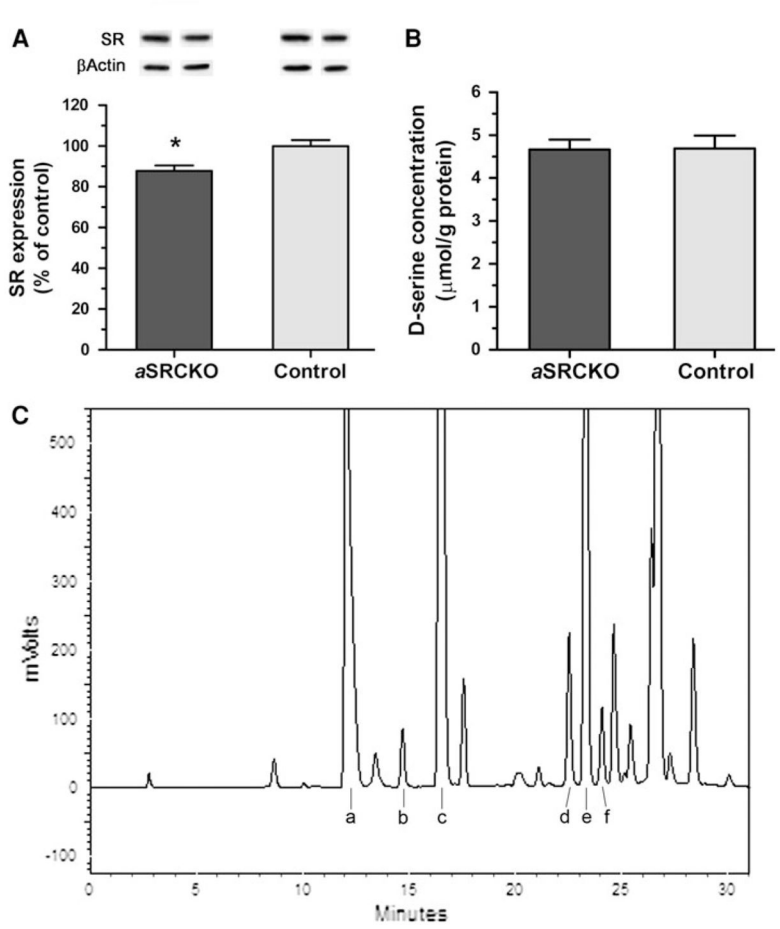

Fig. 2.

Modest reduction in total forebrain SR in *a*SRCKO subjects. Panel **a** shows a 15% reduction SR content found in the forebrain of *a*SRCKO subjects as compared with control (**p* < 0.05, Student's *t* test, *n* = 23–32). Data are expressed as mean percent of control (±SEM). Example immunoblot bands are shown for SR and *β*-actin (loading control) for each genotype. Panel **b** shows the results of HPLC analysis of forebrain D-serine levels. No difference was found between genotypes (*n* = 15). Data are expressed as mean D-serine concentration in μmol/g protein (±SEM). Panel **c** shows an example HPLC chromatogram. Peaks identified by amino acid standards include *a* L-aspartate, *b* L-homocysteic acid (internal standard), *c* L-glutamate, *d* L-serine, *e* L-glutamine and *f* D-serine

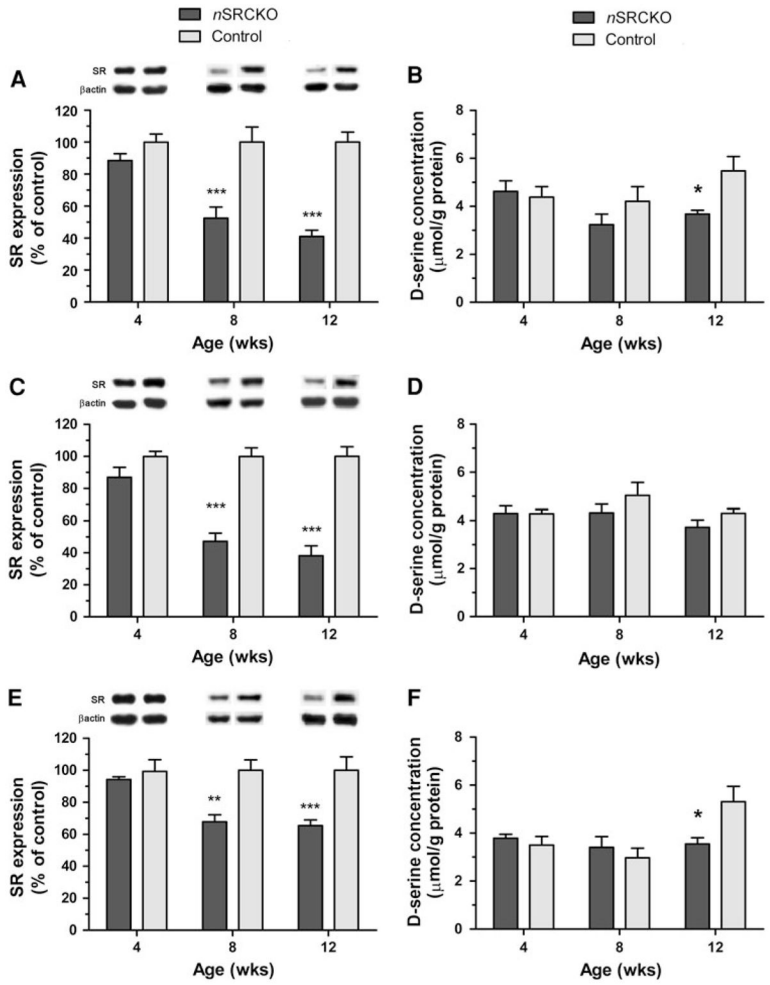

Fig. 3.

SR and D-serine in forebrain subregions of the *n*SRCKO are reduced to a different extent. Changes in SR expression in the frontal cortex, hippocampus and striatum are shown in panels **a**, **c** and **e**, respectively. All SR expression values (SR/*β*-actin) are presented as the percentage of the corresponding (age and brain region) control (±SEM). Significant differences are indicated (**p* < 0.05, ***p* < 0.01, ****p* < 0.001, Bonferroni-corrected post hoc *t* test, *n* = 5–6). Representative immunoblot bands are shown for each condition for SR and *β*-actin. Changes in D-serine tissue homogenate content in the frontal cortex, hippocampus and striatum are shown in panels **b**, **d** and **f**, respectively. Data are expressed as mean D-serine concentration in μmol/g protein (±SEM). Significant differences are indicated as compared with corresponding control (**p* <0.05, Bonferroni-corrected post hoc *t* test, *n* = 5–6)

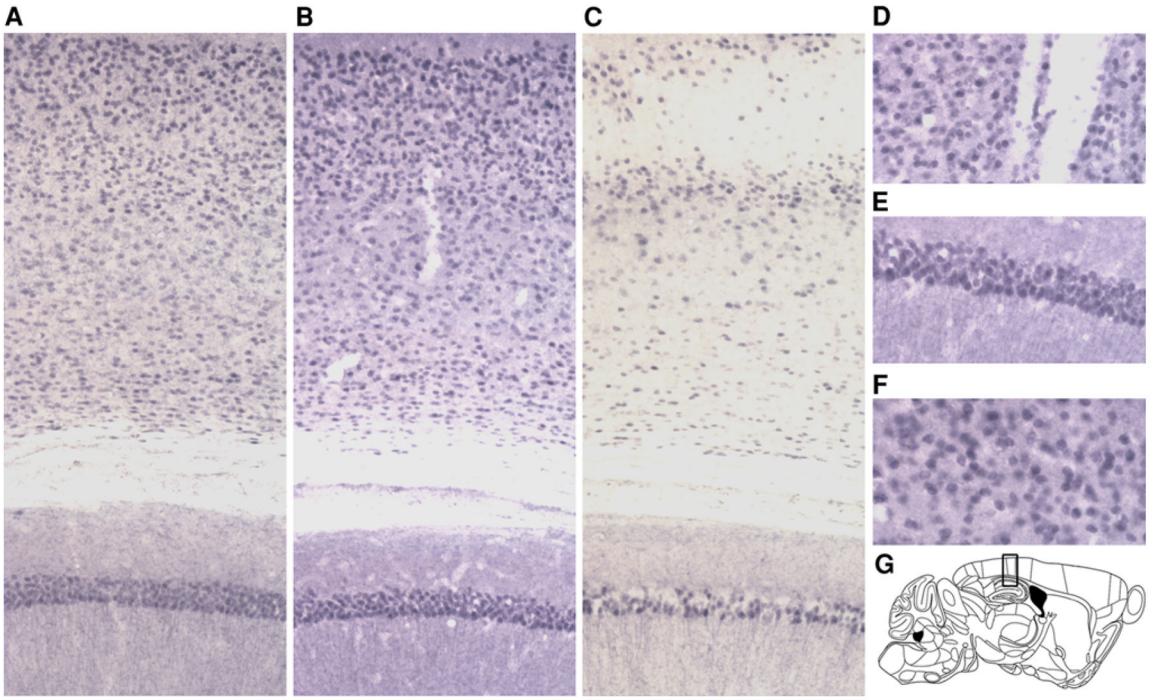

Fig. 4.

Cellular distribution of SR expression in *a*SRCKO, *n*SRCKO and control brains. Light microscopy of SR immunoreactivity in sagittal sections from *a*SRCKO, control (SR fl/fl) and *n*SRCKO mice is shown in panels **a**–**c**, respectively. Each panel is a collage of four images obtained with a ×20 objective. Images show the CA1 region of the hippocampus, corpus callosum and all layers of the parietal cortex (from image *bottom* to *top*). Panel **d** depicts the SR immunoreactivity of the dorsal striatum. Panels **e** and **f** are higher magnification (×40) images of control SR immunoreactivity, showing the principal cell layer of the hippocampus and layers II/III of the cortex, respectively. Panel **g** depicts a mouse brain atlas image (~1.56 mm lateral to midline) that corresponds to the sections shown in **a**, **b** and **c** with the region of analysis indicated by the highlighted rectangle

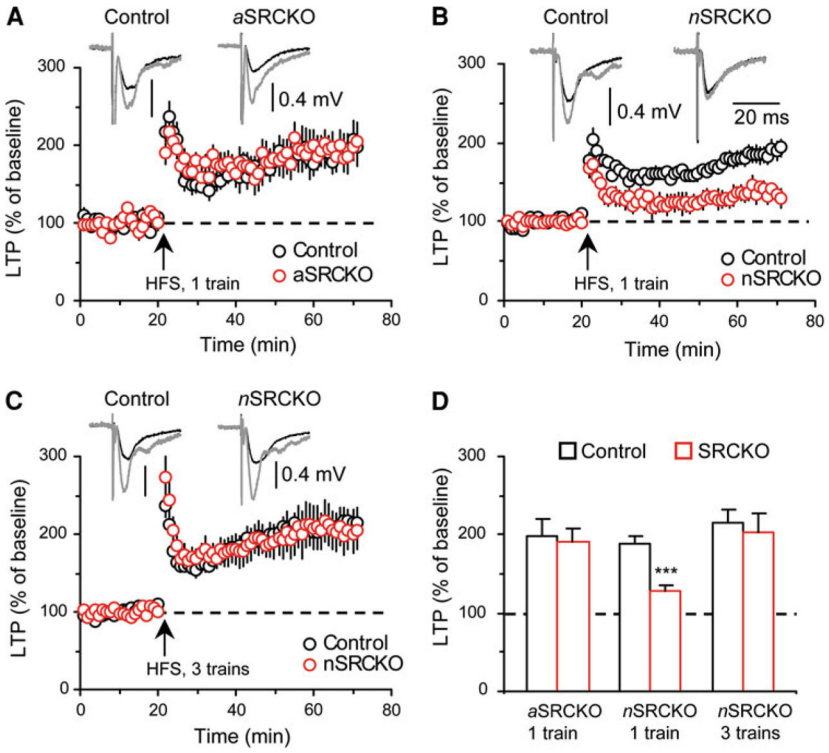

Fig. 5.

LTP at the Schaffer collateral–CA1 synapses in the hippocampus is suppressed in *n*SRCKO but not in *a*SRCKO mice. Panel **a** summary of LTP experiments at the Schaffer collateral–CA1 synapses from four control mice (*n* = 10 slices, *black symbols*) and four *a*SRCKO mice (*n* = 13 slices, *red symbols*). LTP was induced by one 1-s train of high-frequency stimulation (100 Hz, at *arrow*). *Insets* show the average of 10 fEPSPs recorded before (*black traces*) and 45 min after (*gray traces*) the induction of LTP in control and *a*SRCKO mice. Panel **b** summary of LTP experiments from six control mice (*n* = 9 slices) and six *n*SRCKO mice (*n* = 10 slices). LTP was also induced by one 1-s train of high-frequency stimulation (100 Hz, at *arrow*). Panel **c** summary of LTP experiments from five control mice (*n* = 8 slices) and four *n*SRCKO mice (*n* = 9 slices). Here, LTP was induced by three 1-s trains (100 Hz), delivered 20 s apart. Panel **d** summary of all LTP results (from **a** to **c**). Results are presented as means ± SEM. ***p <0.001 (unpaired Student's t test). (Color figure online)

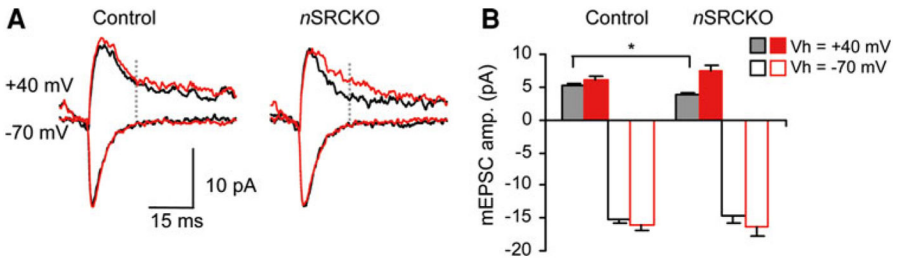

Fig. 6.

Amplitude of the NMDAR mEPSCs is decreased in *n*SRCKO mice. Panel **a**, traces of mEPSCs recorded in CA1 neurons from control or *n*SRCKO mice at −70 mV (*bottom*) and +40 mV (*top*). Traces are averages of 50–150 mEPSCs at each holding potential before (*black traces*) and after (*red traces*) the addition of 10-μM D-serine to external solution. The AMPA receptor-mediated current was measured at the peak of the mEPSCs amplitude at −70 mV. The NMDAR-mediated component of mEPSCs at +40 mV was measured 15 ms after the peak of the AMPAR mEPSCs at −70 mV (at *dashed lines*). Panel **b**, summary plot for experiments as in **a** showing the averaged peak amplitude of the AMPAR mEPSCs at −70 mV (*open bars*) and the amplitude of the NMDAR-mediated component of the mEPSCs at +40 mV (*filled bars*) from four control mice (n = 13 neurons) and four *n*SRCKO mice (n = 10 neurons) under control conditions (*black color*) and in the presence of 10-μM D-serine (*red color*). *p <0.05 (unpaired Student's t test). (Color figure online)

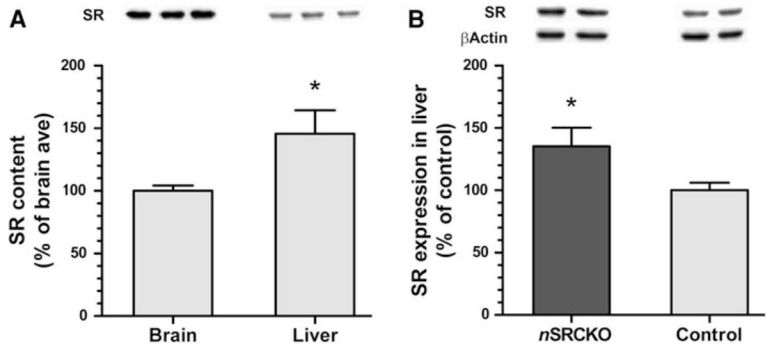

Fig. 7.

SR expression in the liver increases after neuronal deletion. Panel **a** depicts the differences in relative SR content between the brain and liver as determined by immunoblot. Example immunoblots are shown for identical loading amounts (40 μg of protein). Average optical density was then scaled up by factoring in total organ protein content, and is expressed as a percent of brain content (±SEM). Liver contains 46% more SR than brain (*$p < 0.05$, Student's t test, $n = 8$). Panel **b** illustrates the relative SR expression levels in *n*SRCKO and control mice. SR expression (normalized to β-actin) is expressed as a percent of control (±SEM). *n*SRCKO subjects display 35% greater SR expression than control (*$p < 0.05$, Student's t test, $n = 15$)